Original Article

Prenatal enzyme replacement therapy for $Akp2^{-/-}$ mice with lethal hypophosphatasia

Akihiro Hasegawa [a, b], Aki Nakamura-Takahashi [c], Masataka Kasahara [c], Nana Saso [a], Sonoko Narisawa [d], José Luis Millán [d], Osamu Samura [b], Haruhiko Sago [e], Aikou Okamoto [b], Akihiro Umezawa [a, *]

[a] Center for Regenerative Medicine, National Center for Child Health and Development Research Institute, Tokyo, Japan
[b] Department of Obstetrics and Gynecology, The Jikei University School of Medicine, Tokyo, Japan
[c] Department of Pharmacology, Tokyo Dental College, Tokyo, Japan
[d] Sanford Children's Health Research Center, Sanford Burnham Prebys Medical Discovery Institute, La Jolla, CA, USA
[e] Center for Maternal-Fetal, Neonatal and Reproductive Medicine, National Center for Child Health and Development, Tokyo, Japan

ABSTRACT

Hypophosphatasia (HPP) is a congenital skeletal disease. Impairment of bone mineralization and seizures are due to a deficiency of tissue-nonspecific alkaline phosphatase (TNAP). Enzyme replacement therapy (ERT) is available as a highly successful treatment for pediatric-onset HPP. However, the potential for prenatal ERT has not been fully investigated to date. In this study, we assessed outcomes and maternal safety using a combinational approach with prenatal and postnatal administration of recombinant TNAP in $Akp2^{-/-}$ mice as a model of infantile HPP. For the prenatal ERT, we administered subcutaneous injections of recombinant TNAP to pregnant mice from embryonic day 11.5—14.5 until delivery, and then sequentially to $Akp2^{-/-}$ pups from birth to day 18. For the postnatal ERT, we injected $Akp2^{-/-}$ pups from birth until day 18. Prenatal ERT did not cause any ectopic mineralization in heterozygous maternal mice. Both prenatal and postnatal ERT preserved growth, survival rate and improved bone calcification in $Akp2^{-/-}$ mice. However, the effects of additional prenatal treatment to newborn mice appeared to be minimal, and the difference between prenatal and postnatal ERT was subtle. Further improvement of the prenatal ERT schedule and long-term observation will be required. The present paper sets a standard for such future studies.

© 2021, The Japanese Society for Regenerative Medicine. Production and hosting by Elsevier B.V. This is an open access article under the CC BY-NC-ND license (http://creativecommons.org/licenses/by-nc-nd/4.0/).

1. Introduction

Hypophosphatasia (HPP, OMIM #241500) is a rare genetic disease characterized by impairment of systemic bone calcification due to a deficiency of tissue-nonspecific alkaline phosphatase (TNAP). The incidence has been estimated as 1 in 538,000 births in Europe from 2000 to 2009 [1], 1:100,000 in the USA [2] but a bit higher in Japan at 2—3 in 100,000 births [3]. TNAP is one of the critical enzymes for skeletal and dental mineralization. Lack of TNAP causes accumulation of inorganic pyrophosphate (PPi, an inhibitor of mineralization) and depletion of pyridoxal 5′-phosphate (PLP), an active form of vitamin B6 [4—6]. The increase in extracellular PPi leads to rickets/osteomalacia, recurrent fractures, hypoplastic thorax, inadequate mineralization of dentin and enamel, and a lack of acellular cementum. Improper metabolism of vitamin B6 leads to seizures which usually heralds a poor outcome.

HPP is classified into six subtypes based on the time of onset: perinatal severe, prenatal benign, infantile, childhood, adult, and odonto type HPP [7—9]. Symptom of perinatal HPP includes shortening and bowing of fetal tubular bones during the second or third trimester of pregnancy [8,10—12]. Impairment of bone

mineralization starts in utero and, most infants with perinatal severe HPP die at or soon after birth from respiratory insufficiency accompanied by pulmonary hypoplasia [13]. In addition, deficiency of PLP in the brain induces seizures.

Enzyme replacement therapy (ERT) with recombinant mineral-targeted TNAP (asfotase alfa: ENB-0040, Alexion Pharmaceuticals, Cheshire, CT) is effective in these HPP patients as it improves the shortened and bowed tubular bones, extends life expectancy, prevent seizures [14−18] and can be administered right after birth [13]. Furthermore, recombinant TNAP appears able to cross the placenta in mice as per a disclaimer by the manufacturer [19]. In this study, we investigated outcomes and maternal safety using a combinational approach with prenatal and postnatal administration of recombinant TNAP in $Akp2^{-/-}$ mice, a model of infantile HPP.

2. Materials and methods

2.1. Ethical statement

The procedures for performing animal experiments were approved by the Institutional Animal Care and Use Committee of the National Research Institute for Child Health and Development (approval letter number: A2004-004), Japan.

2.2. Experimental design

For maternal analysis, we prepared a prenatal ERT maternal group and a control maternal group. For the prenatal ERT maternal group, we administered subcutaneous injections of recombinant TNAP to the back of the necks of pregnant $Akp2^{+/-}$ heterozygous mice at embryonic day (E) 11.5−14.5. For the control maternal group, Dulbecco's phosphate buffered saline (DPBS) was injected into $Akp2^{+/-}$ heterozygous mice at the same gestation stages. Embryonic days were calculated as E11.5−14.5 from day of mating.

For analysis of 19-day-old pups, we prepared four groups as follows: $Akp2^{+/+}$ mice, untreated $Akp2^{-/-}$ mice, $Akp2^{-/-}$ mice with prenatal and postnatal ERT (prenatal ERT group), and $Akp2^{-/-}$ mice with postnatal ERT (postnatal ERT group). For the prenatal ERT group, pregnant $Akp2^{+/-}$ mice that had been mated with $Akp2^{+/-}$ males were treated with recombinant TNAP starting from the stage of E11.5−14.5 till E18.5 (SC injection, 8.2 mg/kg/day), and their pups received further enzyme treatment (SC injection, 8.2 mg/kg/day) until day 18. For the postnatal ERT group, the mother $Akp2^{+/-}$ mice were not treated with enzyme but their pups received enzyme treatment (SC injection, 8.2 mg/kg/day) until day 18. Genotypes were determined by analyzing DNA from pups' toes just after birth. $Akp2^{+/+}$ and $Akp2^{-/-}$ mice with prenatal ERT, $Akp2^{-/-}$ mice with postnatal ERT were sacrificed on day 19, and untreated $Akp2^{-/-}$ mice were sacrificed between days 17−19 for collection of samples. Asfotase alfa (recombinant mineral-targeted TNAP) was purchased from Alexion Pharmaceuticals.

2.3. Animals and analysis

2.3.1. Lethal type HPP mouse model

The $Akp2^{-/-}$ mice were created by insertion of the Neo cassette into exon 6 of the mouse TNAP gene ($Akp2$) through homologous recombination [20]. All of $Akp2^{-/-}$ mice were fed a rodent diet supplemented with 325 ppm pyridoxine/10 kg of feed (Oriental Yeast Co., Ltd., Tokyo, Japan) to prevent seizures [21]. To identify $Akp2^{-/-}$ homozygotes after birth, we extracted DNA from pup's toe biopsy and performed genotyping by using PCR with the primers as follows: forward, 5′-AGTCCGTGGGCATTGTGACTA-3′; and reverse, 5′-TGCTGCTCCACTCACGTCGAT-3′.

2.3.2. Serum alkaline phosphatase (ALP) activity

For maternal analysis, blood samples were collected from the tail vein with snipping at days for 0 and 3, and the inferior vena cava with a 29-gauge needle after finishing breast feeding was discontinued. Day 0 was defined as the day before initiating subcutaneous injection on E11.5−14.5. Day 3 was defined as E15.5−18.5 before birth. Cessation of breast feeding was defined as more than 4 weeks later after delivery. Maternal mice injected with recombinant TNAP were collected blood samples on the day after cessation of breast feeding (n = 3). Maternal mice injected with DPBS were collected blood samples on the day after cessation of breast feeding (n = 3).

For analysis of 19-day-old pups, blood samples were collected from the inferior vena cava using a 29-gauge needle on day 17−19 after birth. Blood samples of $Akp2^{+/+}$ mice and $Akp2^{-/-}$ mice with prenatal ERT, $Akp2^{-/-}$ mice with postnatal ERT were collected on day 20 after birth, and those of untreated $Akp2^{-/-}$ mice were collected on day 17−19 after birth. We analyzed serum from blood that was centrifuged at 12,000 rpm for 5 min (MX-307, TOMY, Japan). ALP activity was measured by a colorimetric assay. The ALP activity in 1 U was defined as the amount of enzyme needed to catalyze the generation of 1 μmol p-nitrophenol per a minute [22].

2.3.3. Computed tomography (CT) analysis

An *in vivo* CT was used for analysis of the following parameters: bone length, density of cortical, cancellous and total bone, cortical bone area, thickness of cortical bone and minimum moment of inertia of area (Latheta LCT-200; Hitachi Aloka Medical, Japan). Imaging conditions for femur length were as follows: voxel size, 24×48 (μm); slice pitch, 96 μm; rotation angle 360°; the number of shooting direction 1592. Tube voltage, 50 kV; tube current, 0.5 mA. Three-dimensional CT pictures of maternal bones were reconstructed with Amira 5 software (Maxnet Co.,Ltd, Tokyo, Japan). Imaging conditions for maternal bone were as follows: voxel size, 120×480 (μm); slice pitch, 1020 μm; rotation angle 180°; the number of shooting direction 872. Tube voltage, 50 kV; tube current, 0.5 mA.

2.3.4. Histological findings

Neck skin samples of the prenatal ERT mother group were taken on the day after cessation of breast feeding (n = 3). Those of the control mother group were taken on the day after cessation of breast feeding (n = 3). Paraffin sections of neck skin were stained with Carrazi's hematoxylin solution (Muto Pure Chemicals Co., Ltd., Tokyo, Japan) for 5 min and 1% eosin solution (Muto Pure Chemicals Co., Ltd., Tokyo, Japan) for 30 s. Knee joints were fixed in 4% paraformaldehyde, embedded in Super Cryoembedding Medium compound (Leica Microsystems, Wetzlar, Germany) and frozen by using dry ice and hexane without decalcification. Sections (10-μm thickness) were prepared by the Kawamoto film method (Leica Microsystems), air-dried for 20 min, and washed with distilled water [23]. As hematoxylin and eosin (H&E) stain, sections were stained with Carrazi's hematoxylin solution (Muto Pure Chemicals Co., Ltd., Tokyo, Japan) for 5 min and 1% eosin solution (Muto Pure Chemicals Co., Ltd., Tokyo, Japan) for 30 s. As Alcian Blue stain, sections were stained with Alcian Blue solution (pH 2.5) (Muto Pure Chemicals Co., Ltd., Tokyo, Japan) for 30 min, washed with distilled water, and stained with Kernechtrot Stain Solution (Muto Pure Chemicals Co., Ltd., Tokyo, Japan) for 3 min. For ALP enzyme histochemistry, sections were stained with ALP staining kit (Muto Pure Chemicals Co., Ltd., Tokyo, Japan) at 37 °C for 120 min and mounted on glass slides and examined under a light microscope.

2.4. Statistical analysis

Statistical analyses were performed by using Prism 8.01 software (GraphPad, Inc.). Data were expressed as the means ± SEM.
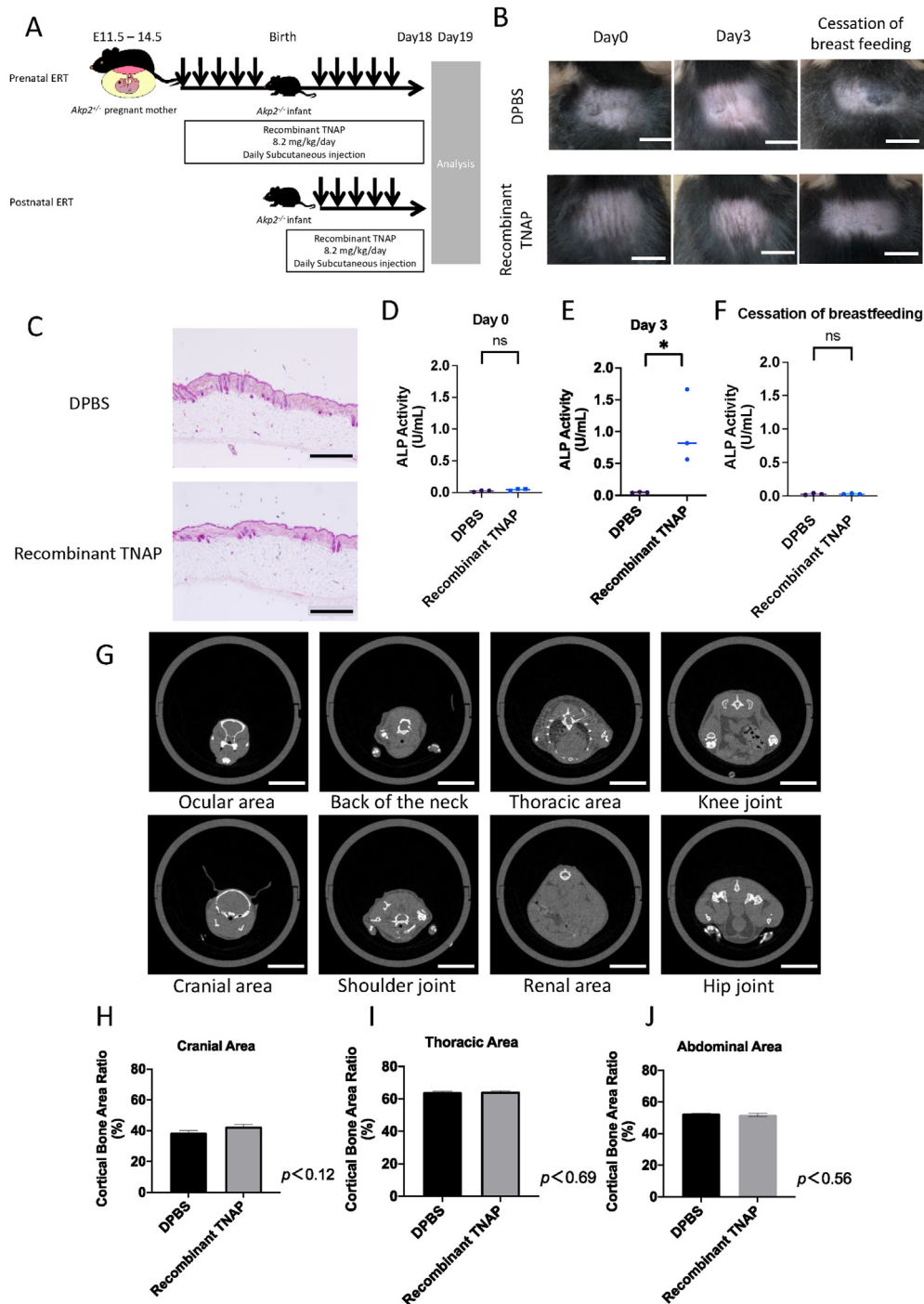
Fig. 1. Experimental design and maternal data. (A) Experimental design of this study. (B) Representative epidermal appearance of injection site in the control mother mice injected with DPBS or the mother mice with prenatal ERT. Scale bars: 100 mm. (C) Histological findings of subdermal skin of injection sites in the control mother mice injected with DPBS or the mother mice with prenatal ERT. Scale bars: 500 μm. Macroscopic and microscopic analyses revealed no inflammation at subcutaneous injection sites in all mother mice. (D) Serum ALP activity of mother mice on day 0, day 3, and the day after cessation of breastfeeding was analyzed in the control mother mice injected with DPBS ($n = 3$) and the mother mice with prenatal ERT ($n = 3$). Data represent the means $\pm$ SE. *$P < 0.05$. (E) Serum ALP activity of mother mice on day 3. (F) Serum ALP activity of mother mice on the day after cessation of breastfeeding. Serum ALP activity significantly increased in the mother mice with prenatal ERT. (G) Two-dimensional images of the ocular area, cranial area, back of the neck, shoulder joint, thoracic area, renal area, knee joint and hip joint in mother mice with prenatal ERT by whole-body CT. Scale bars: 1 mm. We did not detect any ectopic mineralization in the two-dimensional images or video of the whole-body CT (supplementary material). (H) Cortical bone area ratio of cranial area, thoracic area and abdominal area in the control mother mice injected with DPBS ($n = 3$) and mother mice with prenatal ERT ($n = 3$). Data represent the means $\pm$ SE. (I) Cortical bone area ratio of thoracic area. (J) Cortical bone area ratio of abdominal area. We did not find a significant difference in cortical bone area ratios.

Significant differences (p values) between two groups were calculated by using a Student's t test. One-way analysis of variance (ANOVA) was used for multiple comparisons among each group. Survival rate was evaluated by the Kaplan–Meier method, and differences in the survival rates were assessed by the log-rank test.
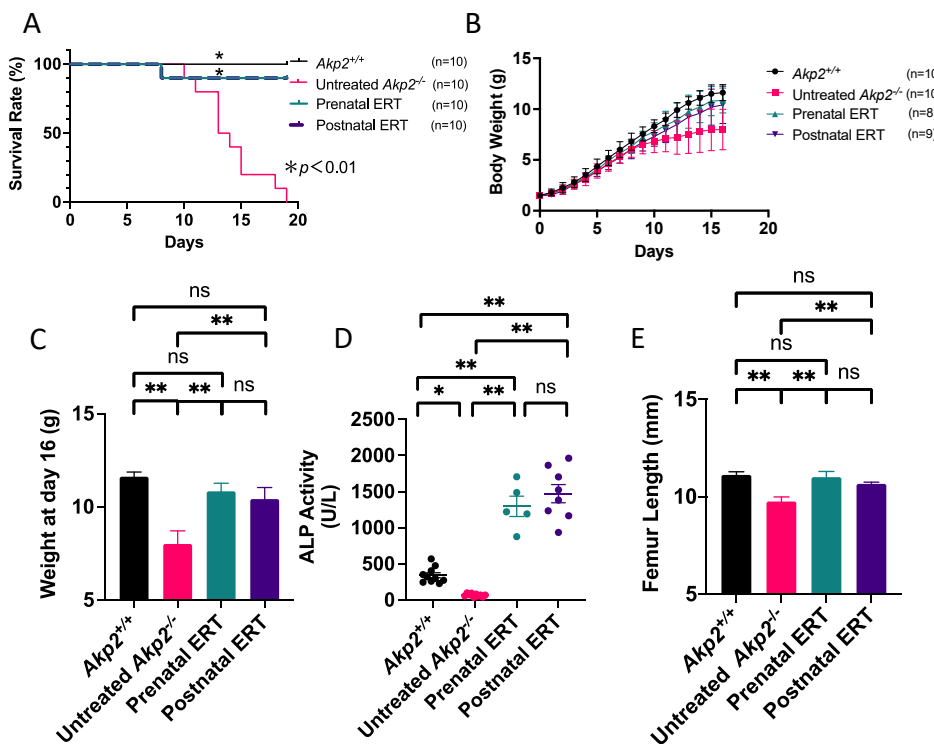
Fig. 2. Prenatal and postnatal ERT prolongs survival and improves growth and femur length in *Akp2*$^{-/-}$ mice. (A) Survival rate of *Akp2*$^{+/+}$ mice ($n = 10$), and untreated *Akp2*$^{-/-}$ mice ($n = 10$), prenatal ERT *Akp2*$^{-/-}$ with TNAP mice ($n = 10$), postnatal ERT *Akp2*$^{-/-}$ with TNAP mice ($n = 10$). (B) Growth curves of *Akp2*$^{+/+}$ mice ($n = 10$), and untreated *Akp2*$^{-/-}$ mice ($n = 10$), prenatal ERT *Akp2*$^{-/-}$ with TNAP mice ($n = 8$), postnatal ERT *Akp2*$^{-/-}$ with TNAP mice ($n = 8$). (C) Body weight on day16, was measured in *Akp2*$^{+/+}$ mice ($n = 10$) and untreated *Akp2*$^{-/-}$ mice ($n = 10$), prenatal ERT *Akp2*$^{-/-}$ with TNAP mice ($n = 8$), postnatal ERT *Akp2*$^{-/-}$ with TNAP mice ($n = 8$). Data represent the means $\pm$ SE. **$P < 0.01$. (D) Serum ALP activity on day 19, was analyzed in *Akp2*$^{+/+}$ mice ($n = 10$), and prenatal ERT *Akp2*$^{-/-}$ with TNAP mice ($n = 5$), postnatal ERT *Akp2*$^{-/-}$ with TNAP mice ($n = 4$), untreated *Akp2*$^{-/-}$ mice ($n = 10$). Data represent the means $\pm$ SE. *$P < 0.05$, **$P < 0.01$. (E) Femur Length on day 19, was measured in *Akp2*$^{+/+}$ mice ($n = 15$), and untreated *Akp2*$^{-/-}$ mice ($n = 9$), prenatal ERT *Akp2*$^{-/-}$ with TNAP mice ($n = 5$), postnatal ERT *Akp2*$^{-/-}$ with TNAP mice ($n = 9$). Data represent the means $\pm$ SE. *$P < 0.05$, **$P < 0.01$.

3. Results

3.1. Analysis of the maternal mice injected with recombinant TNAP

We assessed maternal conditions such as dermal site reaction, ectopic bone calcification, and ALP activity in serum (Fig. 1B—J). Macroscopic and microscopic analysis revealed no inflammation at subcutaneous injection sites in all maternal mice (Fig. 1B and C). Serum ALP activity significantly increased in maternal mice treated with prenatal ERT (Fig. 1D—F). We also assessed ectopic skeletal mineralization in the maternal mice using whole body CT. We did not detect any ectopic mineralization in the two-dimensional images or video of the whole-body CT (Fig. 1G, supplementary material). We compared cortical bone area ratios in cranial, thoracic, and abdominal regions. We did not find significant differences in cortical bone area ratios (Fig. 1H—J).

Supplementary video related to this article can be found at https://doi.org/10.1016/j.reth.2021.06.002

3.2. Prenatal and postnatal ERT improves growth and femur length and prolongs survival in Akp2$^{-/-}$ mice

For the prenatal ERT group, we performed subcutaneous daily injections of recombinant TNAP (8.2 mg/kg) to E11.5—14.5 pregnant *Akp2*$^{+/-}$ mice in the back of the neck. We continued daily subcutaneous injections of recombinant TNAP (8.2 mg/kg) from birth to day 18 to *Akp2*$^{-/-}$ pups. Genotypes were determined by analyzing DNA from the pups' fingers just after birth. For the postnatal ERT group, we injected recombinant TNAP (8.2 mg/kg) to *Akp2*$^{-/-}$ daily

after birth until day 18. We then analyzed *Akp2*$^{+/+}$ ($n = 10$), prenatal ERT ($n = 10$), postnatal ERT ($n = 10$) groups, and the untreated *Akp2*$^{-/-}$ group ($n = 10$). Mice in the *Akp2*$^{+/+}$ group (100%), prenatal ERT group (90%), and postnatal ERT group (90%) survived until day 19. In contrast, all of the untreated *Akp2*$^{-/-}$ mice died between day 10—19 with a median survival of 13.5 days (Fig. 2A). The survival of the prenatal and postnatal ERT groups was significantly prolonged, compared to the untreated *Akp2*$^{-/-}$ mice ($p < 0.01$). Body weights measured at postnatal day 16 of *Akp2*$^{-/-}$ mice with prenatal and postnatal ERT were similar to those in *Akp2*$^{+/+}$ mice (Fig. 2B) compared to the decreased body weight seen in the untreated *Akp2*$^{-/-}$ mice ($p < 0.01$) (Fig. 2C).

Plasma ALP activity on average was as follows; *Akp2*$^{+/+}$ on day 19: 0.3435, prenatal ERT on day 19:1.298, postnatal ERT on day 19:1.473, untreated *Akp2*$^{-/-}$ on day 17—19: 0.06785 U/mL (Fig. 2D). Plasma ALP activity was significantly high in the prenatal and postnatal ERT group than that in the untreated group. Femur length was also improved in the prenatal and postnatal ERT groups on day 19 after birth, compared with the untreated *Akp2*$^{-/-}$ mice on day 17—19 after birth (Fig. 2E).

3.3. Prenatal and postnatal ERT improves bone structure and ALP activity in Akp2$^{-/-}$ mice

We performed a histological analysis of the epiphysis, growth plate, and cortical bone of untreated *Akp2*$^{-/-}$ group on day17—19, prenatal ERT, and postnatal ERT groups on day 19 (Fig. 3). Untreated *Akp2*$^{-/-}$ mice showed abnormal proliferation and irregular arrangement of chondrocytes in the femurs, a defective formation of bone ends in the
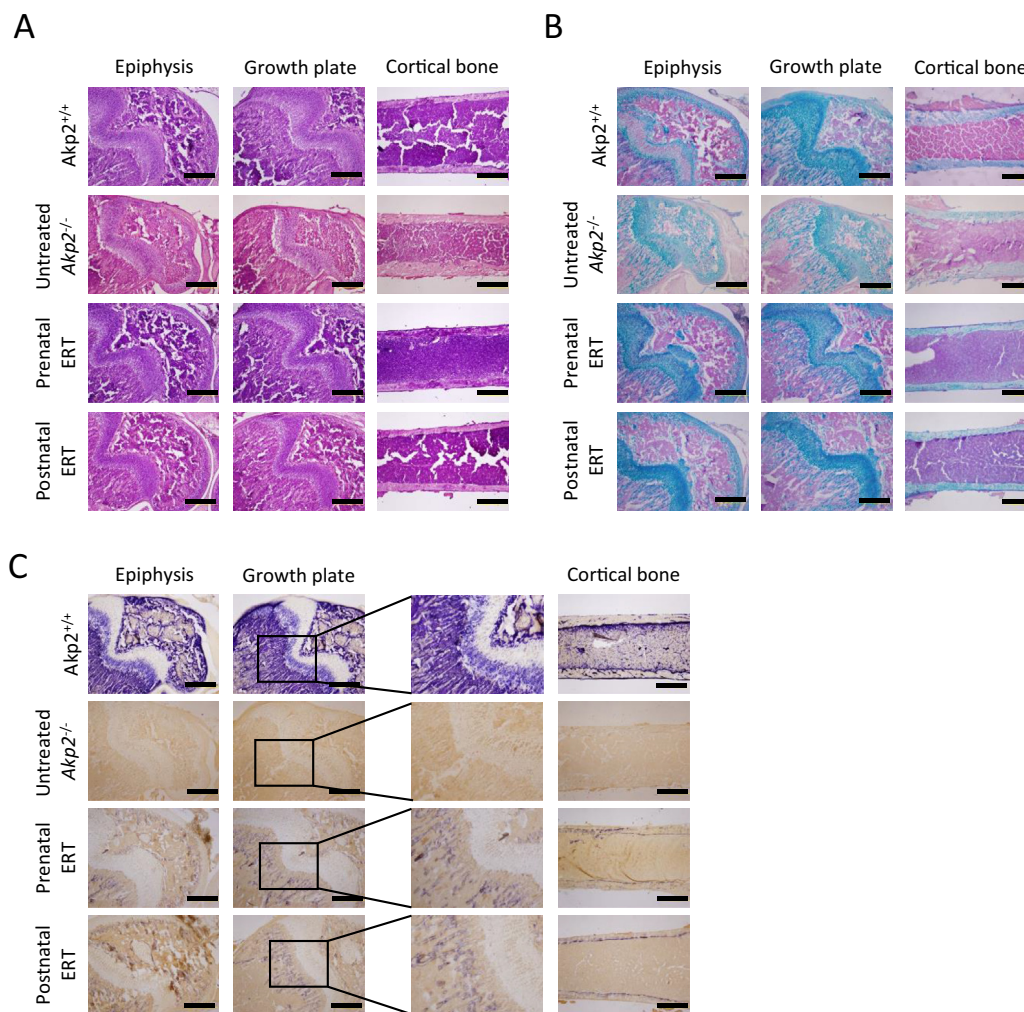
Fig. 3. Histological findings of the effect with prenatal and postnatal ERT to *Akp2$^{-/-}$* mice. Histological findings in *Akp2$^{+/+}$* mice ($n = 15$), and untreated *Akp2$^{-/-}$* mice ($n = 9$), prenatal ERT *Akp2$^{-/-}$* with TNAP mice ($n = 5$), postnatal ERT *Akp2$^{-/-}$* with TNAP mice ($n = 9$). (A) Hematoxylin and Eosin stain (B) Alcian Blue stain (C) Enzyme histochemistry detecting alkaline phosphatase activity.

long axis and inadequate secondary ossification (Fig. 3A and B). Strong ALP activity (as shown in purple) was observed in the trabecular bone and periosteal surface in femurs of *Akp2$^{+/+}$* mice, and no ALP activity was detected in the femurs of untreated *Akp2$^{-/-}$* mice (Fig. 3C). In contrast. ALP activity was present in the growth plate and periosteal periphery of *Akp2$^{-/-}$* mice with prenatal and postnatal ERT (Fig. 3C). These results suggest that prenatal and postnatal ERT are both effective treatment options in *Akp2$^{-/-}$* mice.

3.4. Skeletal morphological analysis by computed tomography

The trabecular bone region of the femur was analyzed by computed tomography (CT) for evaluation of the bone in each group. CT revealed irregular margin of cortical bone, abnormalities in the structure of the growth plate, and low density of cancellous bone in the untreated *Akp2$^{-/-}$* mice (Fig. 4B). Prenatal and postnatal ERT significantly improved cortical bone density in *Akp2$^{-/-}$* mice (Fig. 4C). However, prenatal and postnatal ERT failed to improve cancellous bone density, total bone density, cortical bone area ratio and cortical bone thickness (Fig. 4D–G). Prenatal ERT significantly improved the minimal moment of inertia of area while postnatal ERT was less significantly effective (Fig. 4H).

4. Discussion

ERT is currently the first choice of treatment for pediatric onset HPP. In this study, we assessed the potential efficacy of prenatal ERT using the well-established *Akp2$^{-/-}$* mouse model of infantile HPP. Presumably, starting ERT as early as possible during fetal life would enhance disease prevention for the fetus. Our data indicate that prenatal administration of ERT significantly prevented bone disease, indicating that an early approach to treatment with mineral-targeted TNAP leads better outcomes. Improvements in bone structure, growth and survival observed in our current postnatal ERT are comparable to those of an earlier report with ERT [14]. These improvements were achieved with an approximately 4-fold increase in plasma ALP activity by ERT in the current study. By contrast, ALP activity can be augmented to more than 20- folds using viral vectors for delivery [24–26]. A recent report using higher doses of a viral vector for delivery of mineral-targeted TNAP leading to a 25-fold increase in serum ALP showed evidence of ectopic calcification [24]. However, under the current experimental conditions prenatal ERT did not show any evidence of ectopic calcification.

Improvement of bone structure in the both the prenatal and postnatal ERT groups in this study observed by CT analysis is comparable to the results previously reported using viral vectors
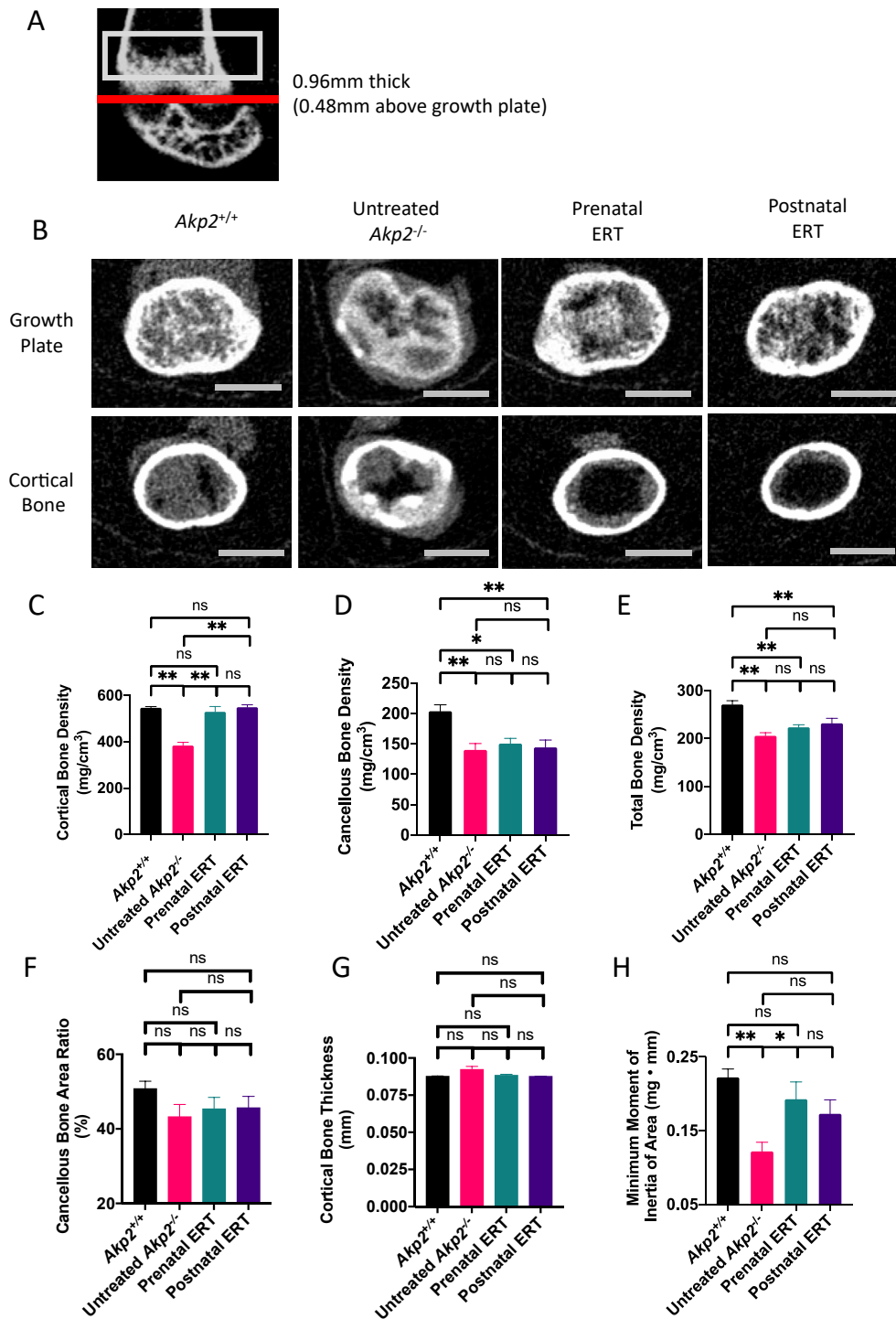
Fig. 4. Comparison of prenatal and postnatal ERT effect by computed tomography analysis. *Akp2*$^{+/+}$ mice ($n = 15$), untreated *Akp2*$^{-/-}$ mice ($n = 9$), prenatal ERT *Akp2*$^{-/-}$ with TNAP mice ($n = 5$), and postnatal ERT *Akp2*$^{-/-}$ with TNAP mice ($n = 9$) were analyzed. Data represent the means ± SE. *$P < 0.05$, **$P < 0.01$. ns: not significant. (A) Images of regions of interest (ROIs) in cancellous bone analysis. (B) Two-dimensional images of growth plate and cortical bone of femurs. Scale bars, 750 μm. (C) Cortical bone density. (D) Cancellous bone density. (E) Total bone density. (F) Cortical bone area ratio. (G) Cortical bone thickness. (H) Minimum Moment of inertia of area.

for delivery [24,26,27]. Improvement of minimum moment of inertia of area with prenatal ERT suggests that reversal of impairment of bone mineralization that is already manifested in fetal life. Indeed, patients with perinatal HPP indeed show symptoms such as shortening and bowing of fetal tubular bones during second or third trimester of pregnancy [8,10–12]. Impairment of bone mineralization starts in utero and, most infants with perinatal HPP

die at or soon after birth from respiratory insufficiency following by pulmonary hypoplasia. In addition, deficiency of PLP in the brain induces seizures that usually herald a poor clinical outcome [28] due to improper gabanergic [29] and purinergic signaling [30] in the central nervous system. An early approach using prenatal ERT with recombinant TNAP may thus lead to earlier alleviation of these seizures. In addition, the craniosynostosis manifested in severely

affected subjects and this condition usually requires multiple surgeries throughout life. In HPP mice, craniosynostosis develops approximately 2 weeks after birth [31] and postnatal ERT with both mineral-targeted [32] and non-targeted ERT [33] prevented craniosynostosis in the $Akp2^{-/-}$ mouse model of HPP. However, in human perinatal HPP, caput membranaceum, wide suture and fontanelles occur rather than the premature fusion of skull bones [12]. Vulnerability develops in utero, and the ultrasonographic findings of soft calvarium is used differentiate diagnosis from any other congenital skeletal dysplasia. The mechanism of progression from caput membranaceum to craniosynostosis is still not clear. However, prenatal ERT may provide a therapeutic avenue to prevent this significant complication of severe HPP disease.

A primary concern of prenatal ERT is maternal safety. The most common side effects of recombinant TNAP are reaction of the injection site with erythema, pruritus, nodule, and pain [18,34,35]. Ectopic calcification, headache, myalgia, irritability, slight fever, hypocalcemia and hyperphosphatemia are also potential side effects. In our experimental settings, prenatal ERT did not show any negative events such as injection site reaction, ectopic skeletal mineralization and inflammation in the maternal mice. Both prenatal and postnatal ERT improved growth, survival rate and bone calcification in $Akp2^{-/-}$ mice. However, the effects of additional prenatal treatment to newborn mice appeared to be minimal, and the difference between prenatal and postnatal ERT was subtle. Further improvement of the prenatal ERT schedule and long-term observation will be required. The present paper sets a standard for such future studies.

Author contribution

AH and AU designed experiments. AH and NS performed experiments. SN and JLM provided materials. AH, NS and AU analyzed data. AH, AT, MK, OS, HS, AO and AU discussed the data and manuscript. AU and AH, SN, JLM contributed to the writing of the manuscript.

Funding

Declaration of competing interest

All authors declare no conflicts of interest or sources of funding.

Acknowledgement

References

[1] Mornet E, Yvard A, Taillandier A, Fauvert D, Simon-Bouy B. A molecular-based estimation of the prevalence of hypophosphatasia in the European population: prevalence of hypophosphatasia. Ann Hum Genet 2011;75:439–45.

[2] Whyte M. Hypophosphatasia. In: Thakker R, Whyte M, Eisman J, Igarashi T, editors. Genetics of bone biology and skeletal disease. Academic Press; 2013. p. 337–60.

[3] Taketani T, Onigata K, Kobayashi H, Mushimoto Y, Fukuda S, Yamaguchi S. Clinical and genetic aspects of hypophosphatasia in Japanese patients. Arch Dis Child 2014;99:211–5.

[4] Russell RG. Excretion of inorganic pyrophosphate in hypophosphatasia. Lancet 1965;2:461–4.

[5] Russell RG, Bisaz S, Donath A, Morgan DB, Fleisch H. Inorganic pyrophosphate in plasma in normal persons and in patients with hypophosphatasia, osteogenesis imperfecta, and other disorders of bone. J Clin Invest 1971;50:961–9.

[6] Whyte MP, Mahuren JD, Vrabel LA, Coburn SP. Markedly increased circulating pyridoxal-5'-phosphate levels in hypophosphatasia. Alkaline phosphatase acts in vitamin B6 metabolism. J Clin Invest 1985;76:752–6.

[7] Mornet E. Hypophosphatasia. Best Pract Res Clin Rheumatol 2008;22(1):113–27.

[8] Wenkert D, McAlister WH, Coburn SP, Zerega JA, Ryan LM, Ericson KL, et al. Hypophosphatasia: nonlethal disease despite skeletal presentation in utero (17 new cases and literature review). J Bone Miner Res 2011;26:2389–98.

[9] Ozono K, Michigami T. Hypophosphatasia now draws more attention of both clinicians and researchers: a commentary on Prevalence of c. 1559delT in ALPL, a common mutation resulting in the perinatal (lethal) form of hypophosphatasias in Japanese and effects of the mutation on heterozygous carriers. J Hum Genet 2011;56:174–6.

[10] Guguloth A, Aswani Y, Anandpara KM. Prenatal diagnosis of hypophosphatasia congenita using ultrasonography. Ultrasonography 2016;35:83–6.

[11] Oyachi M, Harada D, Sakamoto N, Ueyama K, Kondo K, Kishimoto K, et al. A case of perinatal hypophosphatasia with a novel mutation in the ALPL gene: clinical course and review of the literature. Clin Pediatr Endocrinol 2018;27:179–86.

[12] Offiah AC, Vockley J, Munns CF, Murotsuki J. Differential diagnosis of perinatal hypophosphatasia: radiologic perspectives. Pediatr Radiol 2019;49:3–22.

[13] Okazaki Y, Kitajima H, Mochizuki N, Kitaoka T, Michigami T, Ozono K. Lethal hypophosphatasia successfully treated with enzyme replacement from day 1 after birth. Eur J Pediatr 2016;175:433–7.

[14] Millán JL, Narisawa S, Lemire I, Loisel TP, Boileau G, Leonard P, et al. Enzyme replacement therapy for murine hypophosphatasia. J Bone Miner Res 2008;23:777–87.

[15] McKee MD, Nakano Y, Masica DL, Gray JJ, Lemire I, Heft R, et al. Enzyme replacement therapy prevents dental defects in a model of hypophosphatasia. J Dent Res 2011;90:470–6.

[16] Whyte MP, Greenberg CR, Salman NJ, Bober MB, McAlister WH, Wenkert D, et al. Enzyme-replacement therapy in life-threatening hypophosphatasia. N Engl J Med 2012;366:904–13.

[17] Whyte MP, Zhang F, Wenkert D, McAlister WH, Mack KE, Benigno MC, et al. Hypophosphatasia: validation and expansion of the clinical nosology for children from 25 years experience with 173 pediatric patients. Bone 2015;75:229–39.

[18] Reis FS, Gomes DC, Arantes HP, Lazaretti-Castro M. A two-year follow-up of asfotase alfa replacement in a patient with hypophosphatasia: clinical, biochemical, and radiological evaluation. Arch Endocrinol Metab 2020. https://doi.org/10.20945/2359-3997000000222.

[19] European Medicines Agency, Strensiq, INN-asfotase alfa: Annex I Summary of product characteristics. https://www.ema.europa.eu/en/documents/product-information/strensiq-epar-product-information_en.pdf. Accessed November 25, 2020.

[20] Narisawa S, Fröhlander N, Millán JL. Inactivation of two mouse alkaline phosphatase genes and establishment of a model of infantile hypophosphatasia. Dev Dyn 1997;208:432–46.

[21] Négyessy L, Xiao J, Kántor O, Kovács GG, Palkovits M, Dóczi TP, et al. Layer-specific activity of tissue non-specific alkaline phosphatase in the human neocortex. Neuroscience 2011;172:406–18.

[22] Sogabe N, Oda K, Nakamura H, Orimo H, Watanabe H, Hosoi T, et al. Molecular effects of the tissue-nonspecific alkaline phosphatase gene polymorphism (787T > C) associated with bone mineral density. Biomed Res 2008;29:213–9.

[23] Kawamoto T, Kawamoto K. Preparation of thin frozen sections from nonfixed and undecalcified hard tissues using Kawamot's film method (2012). Methods Mol Biol 2014;1130:149–64.

[24] Nakamura-Takahashi A, Tanase T, Matsunaga S, Shintani S, Abe S, Nitahara-Kasahara Y, et al. High-level expression of alkaline phosphatase by adeno-associated virus vector ameliorates pathological bone structure in a hypophosphatasia mouse model. Calcif Tissue Int 2020;106:665–77.

[25] Sugano H, Matsumoto T, Miyake K, Watanabe A, Iijima O, Migita M, et al. Successful gene therapy in utero for lethal murine hypophosphatasia. Hum Gene Ther 2012;23:399–406.

[26] Nakamura-Takahashi A, Miyake K, Watanabe A, Hirai Y, Iijima O, Miyake N, et al. Treatment of hypophosphatasia by muscle-directed expression of bone-targeted alkaline phosphatase via self-complementary AAV8 vector. Mol Ther Methods Clin Dev 2016;3:15059.

[27] Iijima O, Miyake K, Watanabe A, Miyake N, Igarashi T, Kanokoda C, et al. Prevention of lethal murine hypophosphatasia by neonatal ex vivo gene therapy using lentivirally transduced bone marrow cells. Hum Gene Ther 2015;26:801–12.

[28] Whyte MP. Hypophosphatasia - aetiology, nosology, pathogenesis, diagnosis and treatment. Nat Rev Endocrinol 2016;12:233–46.

[29] Waymire KG, Mahuren JD, Jaje JM, Guilarte TR, Coburn SP, MacGregor GR. Mice lacking tissue non-specific alkaline phosphatase die from seizures due to defective metabolism of vitamin B-6. Nat Genet 1995;11:45–51.

[30] Sebastián-Serrano Á, Engel T, de Diego-García L, Olivos-Oré LA, Arribas-Blázquez M, Martínez-Frailes C, et al. Neurodevelopmental alterations and seizures developed by mouse model of infantile hypophosphatasia are associated with purinergic signalling deregulation. Hum Mol Genet 2016;25:4143–56.

[31] Liu J, Nam HK, Campbell C, Gasque Kc da S, Millán JL, Hatch NE. Tissue-nonspecific alkaline phosphatase deficiency causes abnormal craniofacial bone development in the Alpl(-/-) mouse model of infantile hypophosphatasia. Bone 2014;67:81–94.

[32] Liu J, Campbell C, Nam HK, Caron A, Yadav MC, Millán JL, et al. Enzyme replacement for craniofacial skeletal defects and craniosynostosis in murine hypophosphatasia. Bone 2015;78:203–11.

[33] Gasque KCS, Foster BL, Kuss P, Yadav MC, Liu J, Kiffer-Moreira T, et al. Improvement of the skeletal and dental hypophosphatasia phenotype in Alpl-/- mice by administration of soluble (non-targeted) chimeric alkaline phosphatase. Bone 2015;72:137—47.

[34] Kitaoka T, Tajima T, Nagasaki K, Kikuchi T, Yamamoto K, Michigami T, et al. Safety and efficacy of treatment with asfotase alfa in patients with hypophosphatasia: results from a Japanese clinical trial. Clin Endocrinol 2017;87:10—9.

[35] Hofmann CE, Harmatz P, Vockley J, Högler W, Nakayama H, Bishop N, et al. Efficacy and safety of asfotase alfa in infants and young children with hypophosphatasia: a phase 2 open-label study. J Clin Endocrinol Metab 2019;104: 2735—47.